# The Interaction between Rac1 and Its Guanine Nucleotide Dissociation Inhibitor (GDI), Monitored by a Single Fluorescent Coumarin Attached to GDI

Anthony R. Newcombe, Richard W. Stockley, Jackie L. Hunter, and Martin R. Webb*

*National Institute for Medical Research, The Ridgeway, Mill Hill, London, NW7 1AA, U.K.*

*Received December 18, 1998; Revised Manuscript Received March 31, 1999*

ABSTRACT: The interaction of rac with guanine nucleotide dissociation inhibitor protein (rhoGDI) is described, using GDI fluorescently labeled on its single cysteine with *N*-[2-(1-maleimidyl)ethyl]-7-diethylaminocoumarin-3-carboxamide (MDCC). The labeled GDI shows a 70% decrease in fluorescence emission on binding geranylgeranylated rac1·GDP and has an affinity for rac1 within a factor of 2 of the unlabeled GDI. The labeled GDI was used to determine the kinetic mechanism of the interaction by measuring the association and dissociation in real time. The kinetics are interpreted in terms of a two-step mechanism: binding of rac to GDI and then a conformational change of the complex with an overall dissociation constant of 0.4 nM. The conformational change has a rate constant of 7.3 $s^{-1}$ (pH 7.5, 30 °C), and the reverse has a rate constant of $1.4 \times 10^{-3}$ $s^{-1}$. To overcome difficulties inherent in using and manipulating lipid-modified rac, we also used a combination of unmodified rac1, expressed in *Escherichia coli* and produced with C-terminal truncation (thus lacking the cysteine that is the site of lipid attachment), and farnesylated C-terminal peptide. This combination can mimic geranylgeranylated rac1, producing a complex with the coumarin-labeled GDI, and was used to examine the relative importance of different regions of rac1 in interaction with GDI.

Rac is a small G protein with a range of signal-transducing roles within different cell types. Along with other members of the rho family, rho and cdc42, it is involved in control of the cytoskeleton (reviewed by ref *1*). It has an apparently quite separate role, particularly in macrophages, in assembly and control of the NADPH oxidase complex, which forms superoxide in response to bacterial infection (reviewed by ref *2*).

Small G proteins in the rho family interact strongly with a protein, guanine nucleotide dissociation inhibitor, rhoGDI (GDI) (*3*). Although this protein is named because it has the property of strongly inhibiting nucleotide dissociation, its cellular function probably lies elsewhere. For example in quiescent neutrophils (and some other cell types), rac is almost entirely present in the cytosol as a tight complex with GDI. Activation causes dissociation of the rac·GDI complex and movement to the membrane (*4*). The molecular basis for this transfer is not clear, and GDI may function as a control point to keep rac deactivated in the cytosol. Thus nucleotide exchange to a triphosphate may control this translocation (*5*). Understanding how this activation occurs is a long-term goal of the work described here.

Such understanding requires investigation of the molecular interaction between GDI and small G proteins of the rho family, including the mechanism by which the proteins interact and what features of the two proteins are important for binding. Structural studies suggest that this interaction may be complex, as GDI is partly disordered in the absence of bound small G protein (*6*, *7*) and becomes ordered in the rac·GDI complex. To facilitate studies of rac-GDI interaction, we have developed a fluorescence probe on GDI that provides a direct signal for rac binding and so allows us to follow the formation and dissociation of the complex in real time. The probe is a coumarin bound to the single cysteine at position 79 of GDI and was used to investigate GDI interaction with rac1, one of two very similar human rac proteins.

In doing so, we address two problems that have hampered such studies. First, the main signal for interaction has previously been the inhibition of nucleotide exchange and of GAP activation (*3*, *8*, *9*). Both types of inhibition are likely to be due to steric constraints in the complex with GDI and/or the slow dissociation of the complex (see below). However, this property does not produce a direct signal for interaction. Methylanthraniloyl nucleotides complexed to rac (*10*) and GDI with Cys-79 labeled with fluorescein (*7*) have also been used to study the interaction. To provide a direct signal, we have labeled the single cysteine of GDI with a coumarin that shows a large fluorescence change on rac binding to the GDI. This then provides a sensitive measurement of the interaction directly, and we have used this to determine the kinetics of association by rapid reaction techniques to follow the interaction in real time.

For the exploitation of such labeled protein, it is important to have sufficient characterization to show that it is an homogeneous preparation and the extent to which the

* To whom correspondence should be addressed. Tel: (44) 181 959 3666. Fax: (44) 181 906 4477. E-mail: m-webb@nimr.mrc.ac.uk.

[1] Abbreviations: GDI, rho-family guanine nucleotide dissociation inhibitor (rhoGDI); MDCC, *N*-[2-(1-maleimidyl)ethyl]-7-diethylaminocoumarin-3-carboxamide; MDCC-GDI, GDI labeled with MDCC; MDCC-PBP, A197C mutant of the *E. coli* phosphate-binding protein labeled with MDCC; 7-mer, peptide KRKCLLL;12-mer, PVKKRKRKCLLL; mantGDP, 2′(3′)-*O*-methylanthraniloyl-GDP; GMPPNP, guanylylimidodiphosphate.

10.1021/bi9829837 CCC: $18.00 
Published on Web 05/04/1999

labeling modifies its biochemical properties. Inherent in the preparation is the presence of two diastereoisomers as produced by the reaction of the cysteine with the coumarin-maleimide; this reaction is described in detail in the Results. We have experience of this type of labeling particularly with MDCC−PBP, which is the phosphate-binding protein of *Escherichia coli* labeled with the same coumarin-maleimide used here to obtain a fluorescence signal that is sensitive to inorganic phosphate binding (*11*, *12*). We draw on parallels with that system both for the strategy to produce a successful labeled GDI and in its subsequent characterization. In both cases, it seems that the two diastereoisomers have different fluorescence and binding affinities for rac1, and this must be accommodated in the analysis of the results. In practice, for most measurements the signal from the tighter binding diastereoisomer dominates and the weaker binding can be discounted: for the tighter-binding isomer the affinity for rac1 is affected very little by the presence of the coumarin.

The second problem encountered in investigating the interaction with GDI is that rac and its family require lipid modification at the C-terminus in order to interact fully (*8*, *9*). In the cell this modification is geranylgeranylation, and here we use rac1 produced in insect cells using a baculovirus expression system. The full processing of rac1 in eukaryotic cells is the cleavage of the three C-terminal leucines from the protein, following which the newly C-terminal cysteine is carboxymethylated and S-geranylgeranylated. Rac1 expressed in *E. coli* is not modified. Throughout this paper, *E. coli* rac1 is referred to as unmodified and baculovirus rac1 as modified. Unless otherwise stated, the unmodified rac1 is truncated, amino acids 1−184.

Studies with lipid-modified proteins present experimental difficulties in vitro, for example by the need for detergents and difficulties in physical processes such as concentrating. Furthermore, the system is not easily manipulated, for example, precise control of the nucleotide bound to rac. We show that the combination of truncated, unmodified rac1 and farnesylated C-terminal peptide can mimic the geranylgeranylated rac and thereby allow us to test and quantify various features of the rac-GDI interaction. Farnesylation was achieved by reacting the Cys residue of such peptides with farnesyl bromide. The farnesyl group was chosen to modify the peptide because of the ready availability of farnesyl bromide to achieve this chemically and the likelihood that the hydrophobic interaction of GDI with the lipid would not be very specific for the geranylgeranyl group. Hydrophobic interactions have little or no directionality. Here, attempts to farnesylate peptides which terminate at the cysteine were not successful, probably because such peptides are very hydrophilic, containing a group of six basic amino acids. Peptides that include the three leucines were successfully farnesylated, and data are presented using these.

## EXPERIMENTAL PROCEDURES

Human rac1 was obtained from *Spodoptera frugiperda* 9 cells infected with a recombinant baculovirus prepared by Dr. Martin Page (Glaxo-Wellcome). The gene was expressed, and cell membranes containing post-translationally modified rac1 were isolated using standard techniques. The insoluble membrane fraction was resuspended in 50 mL of 20 mM Tris·HCl, pH 7.6, 1 mM $MgCl_2$, and 1 mM phenylmethylsulfonylfluoride, sonicated, and then centrifuged to remove all soluble protein. The membrane pellet was resuspended in this buffer (50 mL) containing 1 mM DTT and 60 mM *n*-octyl glucoside (Sigma), which solubilizes weakly associated membrane bound proteins, and incubated for 1 h at 4 °C. The suspension was centrifuged and the supernatant containing rac1 retained. The supernatant was applied to a Mono-S cation exchange column (1 mL, Pharmacia) equilibrated in 50 mM sodium phosphate, pH 6.5, 1 mM $MgCl_2$, 1 mM DTT, and 30 mM *n*-octyl glucoside. A salt gradient was applied in this buffer from 0 to 1 M NaCl, and the eluted rac1 was stored on ice until required with a typical yield of 1 mg from 2 L of insect cells. Purity of this rac was >95% as determined by SDS−PAGE: this purity was achieved in part during the membrane preparation and extraction resulting in ∼50% purity.

Rac1 was also prepared from *E. coli*. L-broth (100 mL) containing 50 $\mu$g mL$^{-1}$ ampicillin was inoculated with *E. coli* strain JM109 containing the pGEX2T-rac1 plasmid and incubated at 37 °C overnight. An aliquot (10 mL) of this was added to each of eight 500 mL portions of L-Broth (total volume 4 L) containing 50 $\mu$g mL$^{-1}$ ampicillin. The cells were grown with vigorous shaking at 37 °C until an absorbance of 0.8 cm$^{-1}$ at 600 nm was obtained. Expression was induced by the addition of 1 mM IPTG, and the cells grown at 37 °C for a further 4 h. Cells were harvested by centrifugation, and the cell pellet was resuspended in 20 mM Tris·HCl, pH 7.6, and 1 mM $MgCl_2$ (buffer A) containing 1 mM PMSF. The pellet was freeze-thawed and sonicated. The soluble protein fraction was separated from the cell debris by ultracentrifugation and loaded onto a glutathione-Sepharose column (7 mL, Pharmacia) equilibrated in buffer A. The column was then equilibrated with buffer A containing 2.5 mM $CaCl_2$. GST-rac1 fusion protein was cleaved with thrombin while bound to the column. An Antithrombin III agarose column (5 mL, Sigma), equilibrated in buffer A containing 2.5 mM $CaCl_2$, was connected in series to the glutathione-Sepharose column in order to remove the thrombin after cleavage. Buffer A (50 mL) containing 2.5 mM $CaCl_2$ and 500 units of human thrombin (Sigma) was passed at 50 $\mu$L min$^{-1}$. Rac1 was pooled, dialyzed against buffer A, concentrated, and stored at −80 °C. Typical yield is 24 mg of the wild-type protein with purity >95% as determined by SDS−PAGE.

The concentration of rac1 was determined using a calculated extinction coefficient (*13*) of 29 828 M$^{-1}$ cm$^{-1}$. Rac1 from *E. coli* has no post-translational modification and a GSP N-terminus replacing the wild-type methionine: this mutation gives higher solubility. The accidental mutation, F78S (*14*), was removed by standard procedures. When *E. coli* strain JM109 was used, the rac1 was truncated by proteolysis so amino acids 1−184 were obtained (*14*). When BL21 strain was used the protein was full-length. Single-point mutants were prepared using a Stratagene site-directed mutagenesis kit, and sequences were confirmed using dideoxy sequencing (USB Sequenase V2 kit). The molecular mass of the *E. coli* proteins was determined by electrospray mass spectrometry (*15*). The identity of nucleotide bound was determined by HPLC using a Partisil SAX-10 column (Whatman) eluting at 2 mL min$^{-1}$ with 0.5 M $(NH_4)_2HPO_4$, adjusted to pH 4.0 with HCl.

The cDNA of human GDI and the expression vector pRSET A (Invitrogen) were used in order to express full-length GDI in *E. coli*. pRSET A produces a protein that contains an N-terminal polyhistidine fusion tag. Since this tag was not required, it was removed during the subcloning procedure. The GDI cDNA fragment was isolated from the pGEX2T-GDI (*8*), ligated with pRSET A using T4 DNA ligase (Boehringer Mannheim), and then transformed into competent *E. coli* DH5α cells. Recombinant pRSETA-GDI without the polyhistidine tag was prepared using standard techniques and transformed into competent *E. coli* (BL21 strain) for expression. General cloning techniques were performed as described in ref *16*.

L-broth (100 mL) containing 200 $\mu$g mL$^{-1}$ ampicillin was inoculated with BL21 (pRSETA-GDI) cells and grown at 37 °C overnight. This starter culture (10 mL) was added to each of eight 500 mL aliquots of L-broth (total volume 4 L) containing 200 $\mu$g mL$^{-1}$ ampicillin. This was grown to an absorbance at 600 nm of 0.8, and 0.5 mM IPTG was added. The induced cells were grown for a further 3 h, harvested by centrifugation, and resuspended in buffer A plus 1 mM PMSF. The cells were broken by sonication, and the soluble fraction was separated by ultracentrifugation. GDI was purified on a Q-Sepharose column (100 mL, Pharmacia) and equilibrated with buffer A, eluting with a linear salt gradient (1.8 L) in buffer A from 0 to 0.3 M NaCl. Samples of the fractions were analyzed by SDS−PAGE, and those containing GDI were pooled and concentrated. Typical yield was 40−50 mg.

GDI (5 mg) was applied to a 1 mL Mono-Q column, equilibrated in 20 mM Tris·HCl, pH 8.0, and 125 mM NaCl, and eluted with a linear salt gradient in 20 mM Tris·HCl, pH 8.0, and 125−250 mM NaCl. The protein solution was adjusted to pH 7.5, concentrated, and stored at −80 °C. GDI was analyzed by SDS−PAGE, N-terminal amino acid sequencing, and electrospray mass spectrometry. The concentration was measured using the calculated molar extinction coefficient 27 370 M$^{-1}$ cm$^{-1}$ at 280 nm.

GDI (210 $\mu$M) was labeled by stirring with 420 $\mu$M MDCC (*11*) in 20 mM Tris·HCl, pH 8.0, for 45 min at 22 °C. The protein was passed through a 0.2 $\mu$m membrane filter, isolated using a PD10 column (Pharmacia) equilibrated in 20 mM Tris·HCl, pH 7.6, and then stored at −80 °C.

*Trans, trans*-farnesyl bromide (Sigma) was redistilled at low pressure and stored at −80 °C. Peptides, synthesized at NIMR, were labeled in a multiphase reaction mixture containing the following: 10 mM Tris·HCl, 4 mM EDTA, 0.85% (v/v) farnesyl bromide, 8 mg mL$^{-1}$ peptide, and 20% (v/v) dimethyl formamide. The reaction under nitrogen, typically for 7 h, was continually stirred, and the pH was maintained at 8.0 by occasional addition of 1 M Tris base. The extent of reaction was determined by HPLC on a reverse-phase silica column (Whatman Partisil-10 ODS C18, 25 × 0.46 cm). The 40 min gradient was 10% (v/v) acetonitrile, 0.1% trifluoroacetic acid in water, to 60% acetonitrile, 0.1% trifluoroacetic acid, at 1 mL min$^{-1}$. The products were purified on this column, and following concentration, they were stored at −20 °C in 50% (v/v) acetonitrile/water. Mass spectrometry (*15*) confirmed that the peptide had a single farnesyl attached.

Complexes of unmodified rac1 with GTP, GDP, or mantGDP were obtained by exchange of at least a 10-fold excess of the nucleotide with rac1 under conditions which facilitate rapid exchange, excess EDTA over $Mg^{2+}$, typically 40 mM EDTA and 20 mM $(NH_4)_2SO_4$ in 20 mM Tris·HCl, pH 7.6, for 5 min at 30 °C. The protein was isolated on a PD-10 column and the bound nucleotide analyzed by HPLC as described above. For complexes with the nonhydrolyzable analogue GMPPNP, 150 nmol of rac1 was incubated with 600 nmol of GMPPNP and 12 unit alkaline phosphatase linked to agarose beads (Sigma) in 200 mM $(NH_4)_2SO_4$ and 20 mM Tris·HCl, pH 7.6, at 20 °C for 2 h with end-over-end stirring. Samples were analyzed by HPLC as described above. When all of the GDP had been hydrolyzed, the mixture was centrifuged briefly to remove the phosphatase beads and the supernatant was desalted on a PD-10 column.

Experiments using [$^3$H]GDP were quantified using a filter-binding assay, similar to that used previously (*17, 18*), following incubation of 1 $\mu$M rac1 together with varying concentrations of GDI with a 10-fold excess of [$^3$H]GDP in 40 mM EDTA, 20 mM $(NH_4)_2SO_4$, and 20 mM Tris·HCl, pH 7.6, at 30 °C. Note that EDTA accelerates nucleotide exchange. Octylglucoside was present to the extent introduced with modified rac1, typically resulting in 1−2 mM. Exchange of mantGDP was followed using fluorescence energy transfer from rac1 tryptophan(s) to mant with excitation at 290 nm, emission at 440 nm, using the same buffer and equivalent nucleotide and protein concentrations as above.

*Measurements*. Absorbance spectra were obtained on a Beckman DU640 spectrophotometer. Fluorescence measurements were obtained on a Perkin-Elmer LS50B fluorimeter with a xenon lamp. For time-resolved measurements, slit widths were 2.5 nm on the excitation and 5 nm on the emission. Stopped-flow experiments were carried out in a HiTech SF61MX apparatus with a mercury/xenon lamp. There was a monochromator and 5 nm slits on the excitation light at 436 nm and a 455 nm cutoff filter on the emission. Mass spectrometry and tryptic analysis of MDCC-GDI were as previously described (*15*, *19*).

## RESULTS

*Coumarin-Labeled GDI: Characterization*. The single cysteine on GDI was labeled with a range of fluorophores, particularly coumarins that are environmentally sensitive. The resulting molecules were tested to determine if there was a fluorescence change on adding lipid-modified rac1. GDI labeled with the coumarin-maleimide, MDCC (*11*) gave the largest change of those combinations tested, ∼3-fold decrease as shown in Figure 1. Thus, this labeled protein (MDCC-GDI) was characterized further and used in subsequent studies. Absorbance spectroscopy and mass spectral analysis showed that a single molecule of MDCC was covalently bound to GDI. The electrospray mass spectrum of MDCC-GDI gave a mass of 23 490 (±2) Da, 398 greater than that predicted for GDI alone. Previous work (*19*) showed that, under conditions of processing for mass spectrometry, base-catalyzed hydrolysis of the succinimde ring can occur leading to ring opening and producing a mass for the label of 401 Da. However, this unwanted reaction is unlikely to occur to a significant extent under normal labeling conditions (*19*) and use of MDCC-GDI, when the pH remains at ∼8.0 or below. A tryptic digest of MDCC-GDI was analyzed by

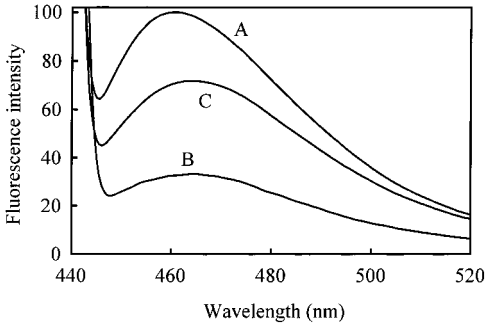


FIGURE 1: Emission spectra of MDCC-GDI. MDCC-GDI (0.1 $\mu$M) was incubated in 20 mM Tris·HCl, pH 7.6, 1 mM $MgCl_2$, 5 $\mu$M BSA, and 1 mM DTT at 21 °C. Emission spectra were measured (A) before and (B) after addition of 0.3 $\mu$M modified rac1, or (C) 5 $\mu$M unmodified rac1 together with 15 $\mu$M farnesyl-12-mer (excitation at 431 nm). Unmodified rac1 or farnesyl-12-mer added on their own gave no fluorescence change.

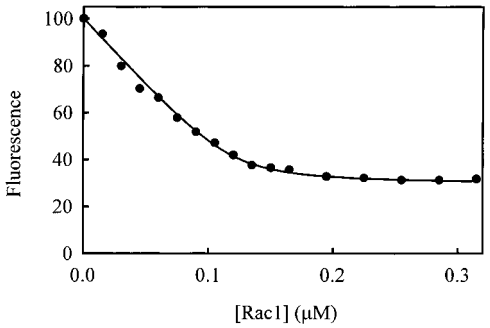


FIGURE 2: Equilibrium binding measurement of rac1·MDCC-GDI interaction. MDCC-GDI (0.2 $\mu$M) was incubated in 20 mM Tris·HCl, pH 7.6, and 1 mM $MgCl_2$ at 30 °C. Aliquots of modified rac1 were added sequentially and the fluorescence emission measured at 457 nm (excitation 431 nm).

HPLC to separate peptides that were then subjected to mass spectrometry (*19*). The only fluorescent species detected have masses of 4536 and 4553 Da, equivalent to that for amino acids 59−79, with either MDCC or the hydrolyzed species present. Again, the basic conditions during the digest are responsible for this partial hydrolysis. These data suggest that the single labeling is on Cys79.

The MDCC-GDI used in subsequent studies is therefore a single molecular species apart from the presence of diastereoisomers, as described below. It was important to show that the labeling has only limited effect on the rac-binding properties of GDI, and this was shown in several ways. A number of measurements described below address this point, and they will be reviewed in the Discussion.

*Diastereoisomers.* A titration of lipid-modified rac1 with MDCC-GDI (Figure 2) produced a linear decrease in fluorescence until ~0.1 $\mu$M rac1, 50% of the total MDCC-GDI concentration. We think that this reflects equal proportions of diastereoisomers of MDCC-GDI, formed when a thiol reacts randomly with either of the two olefinic carbons of the maleimide to produce a chiral center:

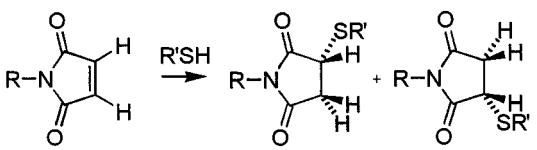


(1)

where R = *N*-[2-(7-diethylaminocoumarin-3-carboxyamido)-ethyl] and R′SH = GDI, attached via Cys-79. There is evidence that maleimides react with protein cysteines in this way, based on analysis of MDCC-labeled phosphate protein (*19, 20*).

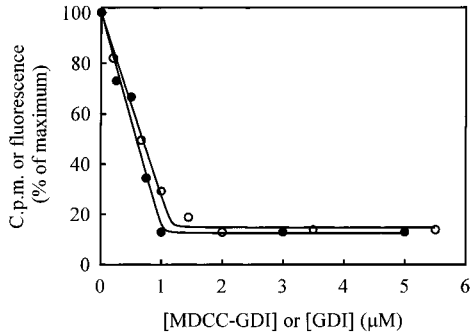


FIGURE 3: Effect of increasing concentration of unlabeled GDI or MDCC-GDI on the ability of modified rac1 to undergo nucleotide exchange. Rac1 (1 $\mu$M) in the presence of GDI was incubated with [$^3$H]GDP (MDCC-GDI, open symbols) or mantGDP (unlabeled GDI, closed symbols) for 10 min, and the extent of exchange was measured as described in Experimental Procedures. The lines are for tight equilibrium binding, allowing the concentration of rac1 to vary to give the best fit: essentially two straight lines that intercept at the concentration of GDI that saturates the rac1. For unlabeled GDI the best fit is at 1.02 $\mu$M, for MDCC-GDI 1.16 $\mu$M.

The titration curve in Figure 2 is consistent with both diastereoisomers binding rac1 but only one dominating the fluorescent change. Further evidence for all of the labeled GDI binding rac1 comes from the titration in Figure 3, described below. This dominant putative diastereoisomer binds the rac1 tightly and is responsible for the linear fluorescence response to ~0.1 $\mu$M. The remaining small fluorescence change (<20% of the total change) occurring from 0.1 to 0.2 $\mu$M is mainly due to the other diastereoisomer, binding rac1 somewhat more weakly. This titration is qualitatively similar to the situation with MDCC-labeled phosphate-binding protein titrated with its ligand $P_i$, for which the implications of diastereoisomers were further discussed (*19*). As a control 3 $\mu$M *E. Coli* rac1, lacking geranylgeranylation, gave no fluorescence change with MDCC-GDI in this concentration range (data not shown). An important conclusion from this titration is that measurements dependent on the coumarin fluorescence to determine rac binding are dominated by the tight binding diastereoisomer, and subsequent analysis will largely assume this by considering a single fluorescence change on rac binding.

*Interaction of MDCC-GDI with Modified rac1.* The relative affinities of MDCC-GDI and unlabeled GDI for modified rac1 were determined by titrating GDI into 0.3 $\mu$M MDCC-GDI·rac1 complex, although a precise treatment of these data was not possible because of the presence of the two diastereoisomers. As measured by fluorescence, 50% of the MDCC-GDI had been displaced from its complex with rac1, and hence there were equal amounts of MDCC-GDI·rac1 and GDI·rac1, when 0.47 $\mu$M GDI had been added. This suggests that the labeling of GDI has very little effect on its affinity for rac1.

The effect of GDI on modified rac1 was measured by the inhibition of nucleotide exchange due to GDI binding, using either mantGDP or [$^3$H]GDP: the presence of coumarin fluorescence interfered with mant fluorescence measurement

and so required the use of radioactivity. A time course of nucleotide exchange in the absence of GDI (data not shown) gave a rate constant for GDP release from the modified rac1 ($1.5 \times 10^{-3}$ s$^{-1}$, 30 °C at 1 mM $Mg^{2+}$) similar to that of unmodified rac1 ($1.1 \times 10^{-3}$ s$^{-1}$). The rate constant for modified rac1 in the presence of excess GDI was $<6 \times 10^{-6}$ s$^{-1}$. This reflects the fact that almost all of this rac1 is bound to GDI and only the small proportion unbound at any time can undergo exchange:

$$\text{GDI·rac1·GDP} \overset{\text{A}}{\rightleftharpoons} \text{GDI} + \text{rac1·GDP} \overset{\text{B}}{\rightleftharpoons} \text{GDI} + \text{rac1} + \text{GDP} \quad (2)$$

$$\text{GDI} + \text{rac1} + \text{GDP*} \rightleftharpoons \text{GDI} + \text{rac1·GDP*} \rightleftharpoons \text{GDI·rac1·GDP*} \quad (3)$$

where GDP* represents radioactively or mant-labeled GDP. This scheme is consistent with the rate constant that we obtain later. The exchange rate of GDP to GDP* in the presence of GDI is controlled by the dissociation of GDI and then GDP (eq 2), as both GDP and GDI binding (eq 3) are fast. If $k_{-GDI}$ and $k_{+GDI}$ are the forward and reverse rate constants for step A and $k_{-GDP}$ is the forward rate constant for step B, the exchange rate constant should be $k_{-GDI}k_{-GDP}/(k_{+GDI} + k_{-GDP})$. $k_{-GDP}$ is $1.5 \times 10^{-3}$ s$^{-1}$, and $k_{-GDI}$ is $1.4 \times 10^{-3}$ s$^{-1}$. At 5.5 $\mu$M GDI, we can approximately use the saturating first-order rate constant, 7.3 s$^{-1}$, for $k_{+GDI}$ (see Figure 5 and text). Thus the exchange rate constant would be $0.29 \times 10^{-6}$ s$^{-1}$.

In practice, a small but variable proportion of baculovirus rac1 (typically 20%, but depending on preparation) does not have its nucleotide exchange inhibited by GDI and thus presumably interacts weakly or not at all with GDI due to damage or lack of proper lipid modification. The effect of different concentrations of unlabeled GDI or MDCC-GDI on rac-nucleotide exchange is shown in Figure 3. In both cases the maximum extent of inhibition is seen at ~1:1 ratio of rac1:GDI. The fact that there is ~15% exchange even at high GDI is due to the portion of "damaged" rac1. This is added evidence that all molecules of MDCC-GDI can bind rac1, but therefore only one diastereoisomer gives a large fluorescence change.

*Kinetic Mechanism of rac1 Binding to GDI*. The fluorescent MDCC-GDI was used to measure the association and dissociation of GDI·rac1 in real time for modified rac1. We use a two-step binding model for interpreting these data, although other models are also possible (see Discussion):

$$\text{MDCC-GDI} + \text{rac1} \overset{1}{\rightleftharpoons} \text{MDCC-GDI·rac1} \overset{2}{\rightleftharpoons} \text{MDCC-GDI*·rac1} \quad (4)$$

Step 2 represents a conformational change that includes the fluorescence change. The equilibrium constant and forward and reverse rate constants for step $i$ are defined as $K_i$, $k_i$, and $k_{-i}$, respectively. Rapid mixing of rac1 with MDCC-GDI in a stopped-flow apparatus allowed the association kinetics to be measured (Figure 4). It was not possible to use high (saturating) rac1 concentrations, because rac1 as prepared was in a high ionic strength solution and it proved impossible to remove salt by dialysis or gel filtration and maintain active protein. Furthermore detergent present in the rac solution became more of a problem at high concentrations, as this affects the fluorescence signal. However, rates were measured at sufficiently high concentrations of rac1 to demonstrate the onset of saturation of the kinetics and to obtain an estimate of $k_2$ (Figure 4b).

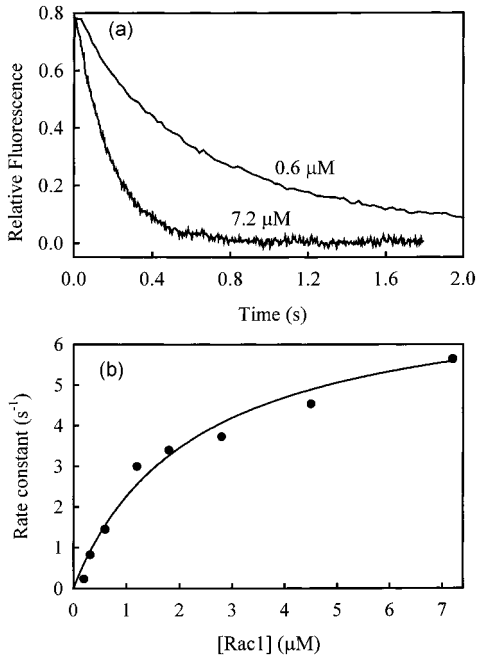


FIGURE 4: Association kinetics of modified rac1 with MDCC-GDI. MDCC-GDI (50 nM) was mixed with a large excess of rac1 and the fluorescence followed with time at 30 °C. (a) Time courses at rac1 concentrations shown. Controls run without rac1 showed a drift in fluorescence, probably due to protein adsorption on surfaces. These were subtracted to give the curves shown, but this correction had little effect on the rate constants: this effect caused a fluorescence amplitude change of 3% of the signal due to rac1 binding in the first 2 s. (b) Dependence of first-order rate constants on rac1 concentration. The data were fit to single exponentials and at least 4 runs averaged at each concentration. The line is the best fit for a two-step binding mechanism (eq 3) where step 1 is assumed rapid, so that the observed rate constant equals $k_2/(1 + [\text{rac1}]K_1) + k_{-2}$. $1/K_1$ is 2.2 $\mu$M and $k_2$ is 7.3 s$^{-1}$. From data in Figure 5, $k_{-2}$ is $1.4 \times 10^{-3}$ s$^{-1}$.

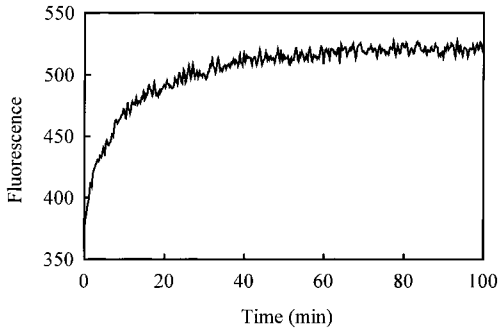


FIGURE 5: Displacement kinetics of MDCC-GDI from its complex with modified rac1 by unlabeled GDI. MDCC-GDI (0.3 $\mu$M) with a small excess of rac1 was incubated with unlabeled GDI (30 $\mu$M). Solution and fluorescence conditions were as in Figure 2. The data shown is after correction for the drift in fluorescence observed when MDCC-GDI alone was incubated for this time period.

Dissociation kinetics were measured by displacing MDCC-GDI from its complex with modified rac1 by mixing with a large excess of unlabeled GDI (Figure 5), and the curve was fit to a single exponential with a rate constant of $1.4 \times 10^{-3}$ s$^{-1}$. The converse measurement, mixing unlabeled GDI·rac1 with excess MDCC-GDI, gave a similar rate constant for unlabeled GDI dissociation ($2.2 \times 10^{-3}$ s$^{-1}$, data not shown).

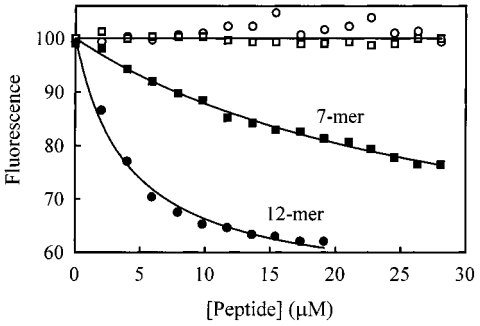


FIGURE 6: Interaction of farnesylated C-terminal peptides with unmodified rac1 and MDCC-GDI. MDCC-GDI (0.3 $\mu$M) was mixed with 2 $\mu$M truncated rac1 (1−184) in 20 mM Tris·HCl, pH 7.6, 1 mM $MgCl_2$, and 1 mM DTT containing 5 $\mu$M BSA at 20 °C. Peptides were titrated into this solution, and the fluorescence emission was measured. Data are corrected for the decrease in fluorescence on addition of similar aliquots of buffer. The peptides were farnesyl-12-mer (filled circles), farnesyl-7-mer (filled squares), 12-mer (open circles), and 7-mer (open squares). The lines are the best fit to binding curves and give a $K_d$ of 4 $\mu$M for the farnesyl 12-mer (fluorescence change 47%) and 31 $\mu$M for the farnesyl 7-mer (49%).

*C-Terminal Peptides of rac1*. To circumvent the problems of working with lipid-modified rac1 to study interaction with GDI, we investigated the possibility of using unmodified rac1 produced in *E. coli*, together with a farnesylated peptide corresponding to the C-terminus of lipid-modified rac1. Three peptides have so far been tested. VKKRKRKC, the C-terminus of the native modified rac (without the C-terminal methylation), failed to react with farnesyl bromide to a significant extent under a range of conditions. This is probably because this peptide is very hydrophilic. In contrast conditions were found to obtain almost quantitative farnesylation of the two other peptides. The 7-mer KRKCLLL is equivalent to amino acids 186−192, the part of *E. coli* rac1 lost on truncation at K184 (*14*), except R185 was omitted to ensure no overlap. The 12-mer PVKKRKRKCLLL extends this sequence across the group of basic amino acids.

Figure 1 shows that there is a fluorescence change on mixing farnesyl-12-mer, truncated unmodified rac1, and MDCC-GDI, suggesting that a complex forms. A series of measurements was done to characterize the interactions: titrations of peptides with MDCC-GDI and rac1 are shown in Figure 6. The 12-mer showed much tighter binding than the 7-mer. The unlabeled peptides produced little or no fluorescence change, as did the farnesyl peptides in the absence of rac. It is worth pointing out here that the fluorescence change may be more a measure of the lipid being present in its pocket on GDI, rather than binding of rac and/or peptide per se. This point is considered in the Discussion. As these controls confirm, the fluorescence change seems to be a measure of the formation of a complex analogous to that between native lipid-modified rac and GDI. To confirm that the unlabeled 12-mer binds only weakly, we showed the binding curve of farnesyl 12-mer to be unaffected by the presence of 15 $\mu$M unlabeled 12-mer. Finally the complex formation was shown to be reversible by addition of excess unlabeled GDI to it. Following mixing 15 $\mu$M farnesyl 12-mer, 0.1 $\mu$M MDCC-GDI, and 0.5 $\mu$M rac1, the addition of 2.5 $\mu$M GDI caused an increase of fluorescence to 99% of that of free MDCC-GDI, suggesting that the labeled GDI was displaced from the complex by the excess unlabeled GDI.

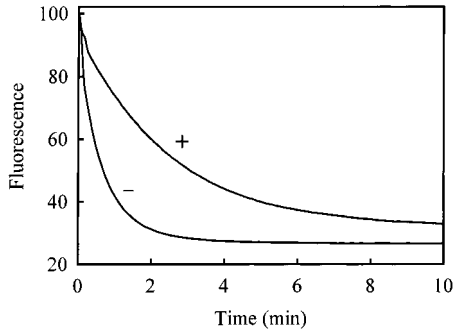


FIGURE 7: Inhibition of rac1-nucleotide exchange by GDI and farnesyl-12-mer. rac1·mantGDP (1 $\mu$M) was incubated at 30 °C with 20 $\mu$M GDP in the presence (+) or absence (−) of 2 $\mu$M GDI and 10 $\mu$M farnesyl-12-mer in 20 mM Tris·HCl, pH 7.6, 1 mM DTT, and 0.5 mM EDTA. The data were fit to single exponentials: $2.5 \times 10^{-2}$ $s^{-1}$ for rac alone and $0.7 \times 10^{-2}$ $s^{-1}$ in the presence of GDI and the peptide.

Table 1: Dissociation Constants for Unmodified rac1 from MDCC-GDI[a]

| rac and peptide | $K_d$ ($\mu$M) |
|---|---|
| rac1·GDP | <0.04[b] |
| rac1·GMPPNP | >10[c,d] |
| rac1·GTP (Q61L) | 1.65 |
| full-length rac1·GDP | 0.14[e] |
| rac1·GDP + unmodified 12-mer | 0.53[e] |
| rac1·GDP with no peptide | >10[c] |
| full-length N-ras·GDP | >20[c,f] |
| Cdc42.GDP (a.a. 1−184) | 0.1 |
| Cdc42.GMPPNP (a.a. 1−184) | >10[c] |

[a] Titrations of rac1 into a solution of 0.1 $\mu$M MDCC-GDI were done equivalent to those in Figure 6. Unless otherwise stated, 15 $\mu$M farnesyl-12-mer was present and the rac1 was truncated (aa 1−184). Fluorescence was corrected by subtracting values using a control of buffer alone with no rac1. The $K_d$ values are an average of at least two determinations. [b] Measurements were at 100 nM MDCC-GDI, so that this value represents an upper limit. Attempts to do the measurements at 30 nM MDCC-GDI did not give reproducible data. [c] No fluorescence change was observed, and this value represents the limit imposed by the errors in the measurement. [d] Rac1·GMPPNP had its nucleotide exchanged back to GDP, and this fully restored binding to MDCC-GDI, showing that the rac1 remained active. [e] These titrations gave an end point with a fluorescence change reduced ~50% relative to rac1·GDP with farnesyl-12-mer (Figure 6). [f] Addition of 0.25 $\mu$M rac1 in the presence of 20 $\mu$M N-ras and the farnesyl peptide showed a full fluorescence change, suggesting that the ras does not inhibit rac1 binding.

Another test of the ternary complex was to return to the effect of bound GDI on rac nucleotide exchange (eqs 2 and 3 and Figure 7). Under conditions where it is predicted that ~75% of the unmodified rac is complexed with GDI, the nucleotide exchange rate was reduced by ~65%. For the ternary complex, we assume that nucleotide exchange cannot occur when unmodified rac is bound to GDI and that dissociation of rac1 is much more rapid than nucleotide exchange of free rac1. All rac1 can undergo exchange, but at a rate reduced by the proportion of rac1 complexed to GDI at any time. Control measurements showed that GDI alone, farnesyl-12-mer alone, or GDI plus unlabeled 12-mer had no effect on the rac1-nucleotide exchange rate.

The farnesyl 12-mer was then used to assess some of the factors that may determine rac1 interaction with GDI. This was done by titrations of rac1 with MDCC-GDI plus farnesyl-12-mer (Table 1). The dissociation constant obtained for truncated unmodified rac1·GDP was <40 nM.

Because this method uses unmodified rac1, it allows precise control of the nucleotide bound in the complex. The above measurements with the peptides used rac1·GDP (aa 1−184). The Leu61 mutant of rac1 has a greatly reduced rate of intrinsic hydrolysis, so that the nucleotide bound in the protein as prepared is >95% GTP. Rac1 bound with the nonhydrolyzable GTP analogue, GMPPNP, was prepared with ~98% nucleotide purity. Thus rac1·GTP (Leu61) and rac1·GMPPNP (wild type) were used to assess the ability of triphosphate-bound rac1 to complex with GDI. In each case the $K_d$ of the rac is greatly increased (Table 1). This suggests that the rac1 in the GTP state does not bind significantly to GDI: the binding that was observed could be explained by the small amount of rac1 with diphosphate bound. Measurements with cdc42 gave similar results.

When full-length unmodified rac1 was titrated in the presence of farnesyl-12-mer, the apparent binding was reduced several-fold relative to truncated rac1 (Table 1) and the total signal change during the titration was reduced. As a control, full-length N-ras showed no binding. Truncated rac on its own showed little or no binding, but weak binding of rac1 with unlabeled 12-mer was observed, again with reduced signal change. This may indicate that the hydrophobic lipid is needed for the full fluorescence change as mentioned above. These results suggest that the identities of amino acids in the C-terminal region of rac1 are important for the specific binding to GDI.

## DISCUSSION

We have investigated the kinetic mechanism of the interaction between rac1 and GDI using two novel techniques. The coumarin-labeled GDI provides a direct fluorescence signal to study the interaction of rac with GDI. We have developed a novel assay using unmodified rac1 together with lipid-modified peptide corresponding to the C-terminus of rac1 that will allow us to probe factors important for the rac-GDI interaction.

It was important to characterize MDCC-GDI fully in order to use it with confidence. MDCC-GDI is a single species, apart from the probable presence of diastereoisomers. So far, fluorescence labels that do not lead to diastereoisomers (e.g., iodoacetamides) have only produced labeled GDI with little or no fluorescence change on binding modified rac. A similar situation was found with PBP labeled with MDCC and related molecules (*19*, *20*). In that case a detailed study including crystal structure allowed us to understand to some extent how the fluorescence change arises and showed a significant difference in environment of the two diastereoisomers. In the case of GDI, equivalent data are not available, but the structure of the C-terminal domain of GDI suggests that the cysteine (and hence the coumarin) is close to the base of the binding pocket suggested for the lipid (*6*, *7*). This may explain the apparent need for a lipid to obtain a full fluorescence change, even after taking into account much weaker binding in the absence of a lipid.

To make use of the signal that responds to the binding of modified rac, it was important for us to show to what extent the presence of the coumarin label affects the rac-binding properties of GDI. The coumarin fluorescence change is dominated by that due to one diastereoisomer, and this is assumed in subsequent analyses. Figure 3 together with the competition binding between unlabeled and labeled GDI suggests that the binding affinity is affected very little. The dissociation kinetics of GDI and MDCC-GDI are also not much different (Figure 5). Thus, we may assume that the kinetic and thermodynamic data obtained using the fluorescent label are similar to that for unmodified GDI.

The kinetics of rac1 association and dissociation were measured in real time and interpreted in terms of the two-step mechanism in eq 3. The conformational change ($k_2$) has a rate constant of 7.3 $s^{-1}$ (pH 7.5, 30 °C), while $1/K_1$ is 2.2 $\mu$M. Modeling the association data, particularly the fact that no lag is observed at any rac concentration, suggests that $k_1 > 3 \times 10^6$ $M^{-1}$ $s^{-1}$ and $k_{-1} > k_2$. This suggests that the measured dissociation rate constant ($1.4 \times 10^{-3}$ $s^{-1}$) is approximately $k_{-2}$. These values give an overall dissociation constant ($K_d$) of 0.4 nM. Because the binding is very tight, $K_d$ is not easily determined from the equilibrium binding data, as such titrations are not practical at the very low concentrations ($\leq K_d$) needed. The preliminary report of a deepening of the lipid-binding pocket on binding of farnesyl peptide (*7*) is a potential structural correlation with the conformation change identified here kinetically.

The combination of a lipid-modified peptide and C-terminally truncated, unmodified rac mimics geranylgeranylated rac in interaction with GDI. An important question is what this approach tells us of the interactions between rac and GDI. The order of binding of peptide and unmodified rac1 to GDI is not established; kinetic data obtained so far do not distinguish between random and ordered addition (A. R. Newcombe and M. R. Webb, unpublished results). There is no evidence of binding of one component in the absence of the other. We will therefore compare the single $K_d$ for modified rac1 binding to GDI with the two individual $K_d$ values for farnesylated peptide binding to GDI in the presence of saturating unmodified rac1 and unmodified rac1 binding to GDI in the presence of saturating farnesylated peptide. In doing so, we will consider the binding in terms of the lipid, the C-terminus of rac1, and "the rest" of rac1.

A striking feature is that the unmodified rac1 in the presence of saturating farnesyl-12-mer binds tightly to GDI, less than 2 orders of magnitude weaker than the modified rac1, the value in the latter case being derived from the kinetic measurements. This suggests that the main bulk of the rac1 molecule has significant interactions with GDI remote from the lipid-binding region. GDI structural data indicate that GDI can be divided essentially into two regions, a well-ordered C-terminal domain containing a lipid-binding pocket and an N-terminal region that is disordered in the absence of bound small G protein (*6*, *7*). This suggests that the interaction is more complex than that of two more-or-less rigid globular proteins, and there may be large areas of well-ordered interactions in the complex with essentially any region of the rac1 structure being involved.

In contrast, the farnesyl peptides in the presence of saturating unmodified rac1 bind much weaker than the modified rac1. Two components that may be factors in this weaker binding are the difference in lipid and the presence of LLL when compared with native, modified rac1. Presumably the smaller farnesyl group sits in the hydrophobic pocket; hydrophobic interactions are generally nonspecific, although the complete surface of the pocket may not be involved. As described above, it seems likely that the full fluorescence change requires the lipid in this pocket.

Several pieces of evidence suggest that the basic amino acids near the C-terminus of rac are important for interaction with GDI. They are conserved between different members of the rho family. The C-terminus seems to bind to GDI in the absence of the lipid, as seen from the titration of unmodified peptide in the presence of rac1 (Table 1). The farnesyl-7-mer, in which the basic amino acid region is incomplete, binds an order of magnitude weaker than the farnesyl-12-mer.

Our data show that guanosine triphosphate complexes of truncated rac are unable to bind tightly to GDI (at least 2 orders of magnitude weaker). Several reports have addressed whether the GTP form of modified rac binds, but with conflicting conclusions: GTP and GDP complexes having similar binding (*8*, *10*) or the GTP complex bind weakly (*9*, *21*). The major technique used in these reports was also titrations, and discrepancies may in part be due to the concentration ranges used. It is technically very difficult to determine $K_d$ values unless the concentration ranges used span that $K_d$ value. An advantage of the technique here is that the concentration ranges can span the observed $K_d$. In the current work, a major aim of using the peptides is to determine the relative importance of the different parts of rac1 in binding. The C-terminal region, represented here by the peptide, contributes to binding, and this contribution may be independent of whether GTP or GDP is bound. This region is not defined in the available structures (ref *14*; M. Hirshberg, A. R. Newcombe, and M. R. Webb, unpublished results). However, once the contribution of the remainder of the rac protein is added, this could result in tight binding of the GDP form and weak binding for the GTP form. Because here the two contributions are separated, the technique is very sensitive to the conformational changes induced by the different nucleotides.

This suggests that regions involved in conformational changes on conversion from GDP to GTP states will be important in determining the binding to GDI. It also seems likely that regions that distinguish the rho family from other small G proteins that do not bind to GDIs will be important. Our results show that unmodified N-ras binds very weakly, if at all, in the peptide assay. The basic C-terminal patch is one such region that differs from ras, but others have been identified from a comparison of rac1 and ras structures, although the overall folds are similar (*14*). The insertion loop present in rac and other rho family members (aa 123−135) is the main gross structural difference from ras. Another difference is at the effector loop, and this may be significant here because of its closeness to the nucleotide-binding site and differences in this loop between the rac·GDP and GMPPNP structures (M. Hirshberg, A. R. Newcombe, and M. R. Webb, unpublished results).

MDCC-GDI should be useful in examining these aspects further. In addition it provides a way to probe for factors that accelerate the dissociation of rac from GDI. The observed dissociation with a half time of several minutes is too slow to explain the action of rac in the cell, in which it begins as a complex with GDI prior to activation. An example is the activation of the NADPH oxidase complex (*22*).

## ACKNOWLEDGMENT

We thank Dr. A. Hall (University College, London) for giving the original *E. coli* expression systems for rac1 and GDI, Dr. M. Page (Glaxo-Wellcome) for the baculovirus expression system for rac1 and assistance in setting up this system, and C. Pickford (NIMR) for N-ras. We thank Dr. M. Hirshberg (Cambridge) for many helpful discussions.

## REFERENCES

1. Symons, M. (1996) *Trends Biochem. Sci. 21*, 178−181.
2. Segal, A. W., and Abo, A. (1993) *Trends Biochem. Sci. 18*, 43−47.
3. Ueda, T., Kikuchi, A., Ohga, N., Yamamoto, J., and Takai, Y. (1990) *J. Biol. Chem. 265*, 9373−9380.
4. Quinn, M. T., Evans, T., Loetterle, L. R., Jesaitis, A. J., and Bokoch, G. M. (1993) *J. Biol. Chem. 268*, 20983−20987.
5. Bokoch, G. M., Bohl, B. P., and Chuang, T. (1994) *J. Biol. Chem. 269*, 31674−31679.
6. Keep, N. H., Barnes, M., Barsukov, I., Badii, R., Lian, L., Segal, A. W., Moody, P. C. E., and Roberts, G. C. K. (1997) *Structure 5*, 623−633.
7. Gosser, Y. Q., Nomanbhoy, T. K., Aghazadeh, B., Manor, D., Combs, C., Cerione, R. A., and Rosen, M. K. (1997) *Nature 387*, 814−819.
8. Hancock, J. F., and Hall, A. (1993) *EMBO J. 12*, 1915−1921.
9. Chuang, T. H., Xu, X., Knaus, U. G., Hart, M. J., and Bokoch, G. M. (1993) *J. Biol. Chem. 268*, 775−778.
10. Nomanbhoy, T. K., and Cerione, R. A. (1996) *J. Biol. Chem. 271*, 10004−10009.
11. Corrie, J. E. T. (1994) *J. Chem. Soc., Perkin Trans. 1*, 2975−2982.
12. Brune, M., Hunter, J., Corrie, J. E. T., and Webb, M. R. (1994) *Biochemistry 33*, 8262−8271.
13. Gill, S. C., and von Hippel, P. H. (1989) *Anal. Biochem. 182*, 319−326.
14. Hirshberg, M., Stockley, R. W., Dodson, G., and Webb, M. R. (1997) *Nat. Struct. Biol. 4*, 147−152.
15. Aitken, A., Howell, S., Jones, D., Madrazo, J., and Patel, Y. (1995) *J. Biol. Chem. 270*, 5706−5709.
16. Sambrook, J., Fritsch, E. F., and Maniatis, T. (1989) *Molecular cloning. A laboratory manual*, 2nd ed., Cold Spring Harbor Laboratory Press, Cold Spring Harbor, NY.
17. Hall, A., and Self, A. J. (1986) *J. Biol. Chem. 261*, 10963−10965.
18. Neal, S. E., Eccleston, J. F., Hall, A., and Webb, M. R. (1988) *J. Biol. Chem. 263*, 19718−19722.
19. Brune, M., Hunter, J. L., Howell, S. A., Martin, S. R., Hazlett, T. L., Corrie, J. E. T., and Webb, M. R. (1998) *Biochemistry 37*, 10370−10380.
20. Hirshberg, M., Henrick, K., Haire, L. L., Vasisht, N., Brune, M., Corrie, J. E. T., and Webb, M. R. (1998) *Biochemistry 37*, 10381−10385.
21. Sasaki, T., Kato, M., and Takai, Y. (1993) *J. Biol. Chem. 268*, 23959−23963.
22. Abo, A., Webb, M. R., Grogan, A., and Segal, A. W. (1994) *Biochem. J. 298*, 585−591.

BI9829837